

Importance of subleading corrections for the Mott critical point

¹Patrick Sémon and ^{1,2}A.-M.S. Tremblay

¹*Département de physique and Regroupement québécois sur les matériaux de pointe, Université de Sherbrooke, Sherbrooke, Québec, Canada J1K 2R1 and*

²*Canadian Institute for Advanced Research, Toronto, Ontario, Canada, M5G 1Z8*

The interaction-induced metal-insulator transition should be in the Ising universality class. Experiments on layered organic superconductors suggest that the observed critical endpoint of the first-order Mott transition belongs instead to a different universality class. To address this question, we use dynamical mean-field theory and a cluster generalization that is necessary to account for short-range spatial correlations in two dimensions. Such calculations can give information on crossover effects, in particular quantum ones, that are not included in the simplest mean-field. In the cluster calculation, a canonical transformation that minimizes the sign problem in continuous-time quantum Monte Carlo calculations allows us to obtain very accurate results for double occupancy. These results show that there are important subleading corrections that can lead to apparent exponents that are different from mean-field. Experiments on optical lattices could verify our predictions.

Half-filled band materials should be metallic, but they are sometimes insulators [1]. This paradox was discussed by Boer and Verwey and by Peierls as early as 1937, but the first theoretical advance came from Mott in 1949. He found that as a function of some external parameter, it is possible to control the ratio of interaction energy to kinetic energy and drive the system through a metal-insulator transition. This Mott transition has by now been clearly identified in a few materials [1] and in optical lattices of cold atoms [2, 3]. The order parameter for the interaction-induced transition should be in the Ising universality class [4–6], with no breaking of translational or rotational invariance. This has been verified explicitly in the three-dimensional compound V_2O_3 [7].

It thus came as a surprise when it was discovered that in two-dimensional layered κ -ET organic superconductors [8], critical exponents for the Mott critical point, measured in both charge (conductivity) [9] and spin (NMR) channels [10], appear to belong to a different universality class. Several proposals have appeared to explain this result. Imada *et al.* [11, 12] suggested that while the high-temperature regime is described by classical Ising exponents, there is also a continuous transition at $T = 0$ and, in between, a marginal quantum critical point that controls the observed behavior. Papanikolaou *et al.* [13] instead started from the 2d-Ising universality class and argued that, away from criticality, the subleading energy exponent dominates for the conductivity over the leading order parameter exponent. The latter becomes relevant only very close to T_c . A recent experiment on thermal expansion coefficient finally, argues that the Ising universality class is the correct one [14]. That finding disagrees with the latest theoretical calculation [15] performed with Cluster Dynamical Mean-Field theory (CDMFT) [16, 17] that measured an exponent $\delta = 2$ in agreement with the above-mentioned conductivity [9] and NMR experiments [10].

Here we revisit the critical behavior at the Mott critical endpoint by studying the one-band Hubbard model, the

simplest model of interacting electrons that contains the physics of the Mott transition. We use single-site Dynamical Mean-Field Theory (DMFT) [18–20] and CDMFT. Single-site DMFT is exact in infinite dimension and can be applied to lower-dimensional lattices [21, 22]. While it can be proven analytically [5] that for DMFT the behavior is mean-field like, the possibility of quantum critical transients, the size of the critical region and the precise value of the exponents have not been verified numerically. This is important since there could be an unstable quantum critical point controlling the behavior in the experimentally accessible regime, as has already been observed for the conductivity [23]. The same question arises with CDMFT that takes into account the momentum dependence of the self-energy, a physical ingredient that is known to be important in two dimensions [24–35]. Since the Mott transition occurs far above long-ranged ordered ground states, CDMFT should be an accurate description of the organics, except asymptotically close to the transition where the usual critical fluctuations should take over mean-field behavior.

Although this problem has already been studied with these methods, improvements in computer performance and in algorithms allow us to obtain much more accurate data. In the case of CDMFT, for the frustrated lattice considered here, the sign problem in the Continuous Time Quantum-Monte Carlo solution of the Hybridization expansion (CT-HYB) [36–39] is minimized by a canonical transformation. This allows us to approach the critical point ten times closer in reduced pressure than previously possible.

Method: The simplest model that contains both the strong on-site Coulomb repulsion and the kinetic energy of the frustrated κ -ET's lattice, is the half-filled Hubbard model on a 2D anisotropic triangular lattice

$$H = \sum_{ij\sigma} (t_{ij} - \delta_{ij}\mu) c_{i\sigma}^\dagger c_{j\sigma} + U \sum_i n_{i\uparrow} n_{i\downarrow}, \quad (1)$$

where $c_{i\sigma}^\dagger$ creates a spin σ electron at site i , $n_{i\sigma} = c_{i\sigma}^\dagger c_{i\sigma}$

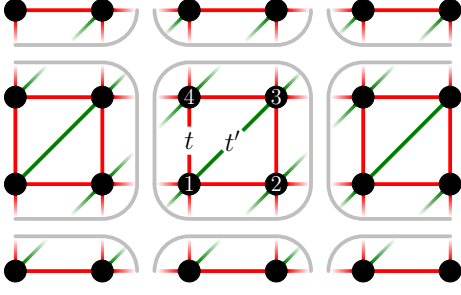


FIG. 1: Periodic partitioning of the anisotropic triangular lattice into 2×2 plaquettes for CDMFT.

is the spin σ density at site i , $t_{ij} = t_{ji}^*$ are the hopping amplitudes as shown in Fig. (1) while μ and U are, respectively, the chemical potential and the screened Coulomb repulsion.

We use single-site DMFT [21] and its cluster extension CDMFT [16, 17] to solve the Hamiltonian Eq.(1). These methods start with a periodic partitioning of the infinite lattice model into independent sites (DMFT) or clusters (CDMFT). The missing environment of the cluster is replaced by a bath of non-interacting electrons. The action of the cluster in a bath model may be written as

$$S = S_{\text{cl}}(\mathbf{c}^\dagger, \mathbf{c}) + \int_0^\beta d\tau d\tau' \mathbf{c}^\dagger(\tau') \mathbf{\Delta}(\tau' - \tau) \mathbf{c}(\tau), \quad (2)$$

where S_{cl} is the cluster-action as obtained by the partitioning, \mathbf{c} the column vector of the corresponding $c_{i\sigma}$'s and the bath has been integrated out in favor of a hybridization function $\mathbf{\Delta} = (\Delta_{i\sigma, j\sigma'})$. This defines an effective impurity model. Approximating the unknown lattice self-energy locally by the impurity self-energy Σ' and using Dyson's equation, the lattice Green's function reads

$$\mathbf{G}'_{\text{lat}}^{-1} = \mathbf{G}_{0, \text{lat}}^{-1} - \Sigma', \quad (3)$$

with $\mathbf{G}_{0, \text{lat}}$ the non-interacting lattice Green's function. The hybridization function $\mathbf{\Delta}$ is determined self-consistently from the requirement that the impurity Green's function computed from the action Eq. (2) coincides with the projection of the approximate lattice Green's function \mathbf{G}'_{lat} on the impurity cluster. This self-consistency condition may be derived from a variational principle [40]. For CDMFT we take the 2×2 plaquette illustrated in Fig. (1). This accounts at least locally for the geometrical frustration in the κ -ET.

To obtain the impurity Green's function (and other observables), we use a continuous time quantum Monte-Carlo (CTQMC) solver [36–39]. This method starts with a diagrammatic expansion of the impurity partition function in powers of the hybridization function. The key idea is then to recombine, for a given 'cluster-vertex', all possible contractions over the bath (i.e. the hybridization function) by a determinant before summing up the series by Monte-Carlo sampling. Without this recombination

of diagrams the fermionic sign problem would be fatal [36].

In the case of CDMFT, symmetries of the problem can be used to speed up the simulation by choosing a single particle basis in Eq. (2) that transforms according to the irreducible representations [39]. In our case, separate charge conservation of $\sigma = \uparrow, \downarrow$ particles and the C_{2v} point group symmetry of the anisotropic plaquette lead to the single particle basis (see Fig. 1 for indices)

$$\begin{aligned} c_{A_1\sigma} &= \frac{1}{\sqrt{2}}(c_{1\sigma} + c_{3\sigma}) & c'_{A_1\sigma} &= \frac{1}{\sqrt{2}}(c_{2\sigma} + c_{4\sigma}) \\ c_{B_1\sigma} &= \frac{1}{\sqrt{2}}(c_{1\sigma} - c_{3\sigma}) \\ c_{B_2\sigma} &= \frac{1}{\sqrt{2}}(c_{2\sigma} - c_{4\sigma}), \end{aligned} \quad (4)$$

with A_1, B_1 and B_2 irreducible representations of C_{2v} (A_2 is empty). Due to the degeneracy in the A_1 subspace, there is a degree of freedom in the choice of basis which may be parameterized by an angle θ as follows,

$$\cos\theta c'_{A_1\sigma} - \sin\theta c_{A_1\sigma}, \quad \sin\theta c'_{A_1\sigma} + \cos\theta c_{A_1\sigma}. \quad (5)$$

In this basis the hybridization function $\mathbf{\Delta}$ takes a block-diagonal form with one 2×2 block (A_1) and two 1×1 blocks (B_1 and B_2) for each spin (in the normal phase). The sign problem in the Monte Carlo simulation shows a strong dependence in θ as shown in Fig. 2 for $t/t' = 0.8$, $\beta = 20$ and different values of U . One can check that the maximum of the average sign is related to the angle θ that minimizes the off-diagonal elements of the hybridization function (A_1 block) with respect to some norm. The dots in the inset of Fig. 2 indicate the maximum with respect to L_1 and L_2 on $[0, \beta]$. The usual basis, $\theta = 0$, has a bad sign problem.

To analyze our results, we derive subleading corrections to mean-field theory. The singular part of the mean-field equation for the order parameter η takes the form [5, 41]

$$p\eta + c\eta^3 = h \quad (6)$$

with c a constant, while p and h are defined by $p \equiv p_1(U - U_c) + p_2(T - T_c)$ and $h \equiv h_1(U - U_c) + h_2(T - T_c)$. Like in the liquid-gas transition, interaction strength and temperature are not in general eigendirections, which explains the way they appear in p and h . When $p = 0$, the solution is $\eta = (h/c)^{1/\delta}$, which defines $\delta = 3$. Approaching the critical line along $\delta U \equiv (U - U_c)$ for example, the mean-field Eq.(6) takes the form

$$p_1\delta U\eta + c\eta^3 = h_1\delta U. \quad (7)$$

One can show that the general solution of that equation is of the form

$$\eta = \sum_{i=1}^{\infty} \delta U^{i/3} \eta_i. \quad (8)$$

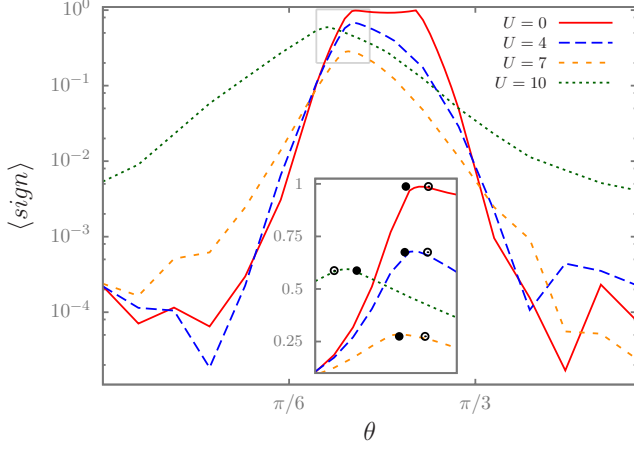


FIG. 2: Average sign in CTQMC simulations of the anisotropic plaquette impurity problem at CDMFT self-consistency with $t/t' = 0.8$ ($t \equiv 1$) and $\beta = 20$ as a function of the angle θ in Eq. 5 for different values of U . The inset zooms on the region where the sign takes its maximum, as indicated. The dots associated with each curve indicate the angle where the off-diagonal elements of the corresponding hybridization functions are minimal with respect to the L_1 norm (filled) and the L_2 norm (empty).

with expansion coefficients η_i . The first term, $\delta U^{1/3}$, and the subleading correction, $\delta U^{2/3}$, are the only terms that lead to an infinite first derivative at the critical point. In the case of DMFT, η is the singular part of the hybridization function.

In the following we compute double occupancy $D \equiv \langle n_{\uparrow} n_{\downarrow} \rangle$. Double occupancy in general should be a smooth function of η that can be expanded as a power series, a result that can be proven in DMFT [5]. Hence, even when η is dominated by the leading term $\delta U^{1/\delta}$, the η^2 term of the power series leads to subleading $\delta U^{2/\delta}$ corrections.

For the single-band Hubbard model, singular behavior of D implies singular behavior in both spin and charge channels [5], as follows from the following two sum rules on spin, χ_{sp} , and charge, χ_{ch} , susceptibilities, $T \sum_n \int \frac{d^2 q}{(2\pi)^2} \chi_{sp}(\mathbf{q}, \omega_n) = n - 2D$ and $T \sum_n \int \frac{d^2 q}{(2\pi)^2} \chi_{ch}(\mathbf{q}, \omega_n) = n + 2D - n^2$ where ω_n are Matsubara frequencies and \mathbf{q} wave vectors in the Brillouin zone.

Below the critical temperature, there is a first-order transition with a jump in double occupancy that scales like p^β with $\beta = 1/2$. It is very difficult to obtain this exponent numerically because of hysteresis. Similarly, the exponent for the susceptibility $(\partial \eta / \partial h)_p \sim p^{-\gamma}$ with $\gamma = 1$ requires numerical differentiation and cannot be obtained accurately.

Results: Figure 3 displays double occupancy as a function of interaction strength calculated for both single-site DMFT (blue squares) and CDMFT (red circles) at our best estimate of the corresponding critical temperatures.

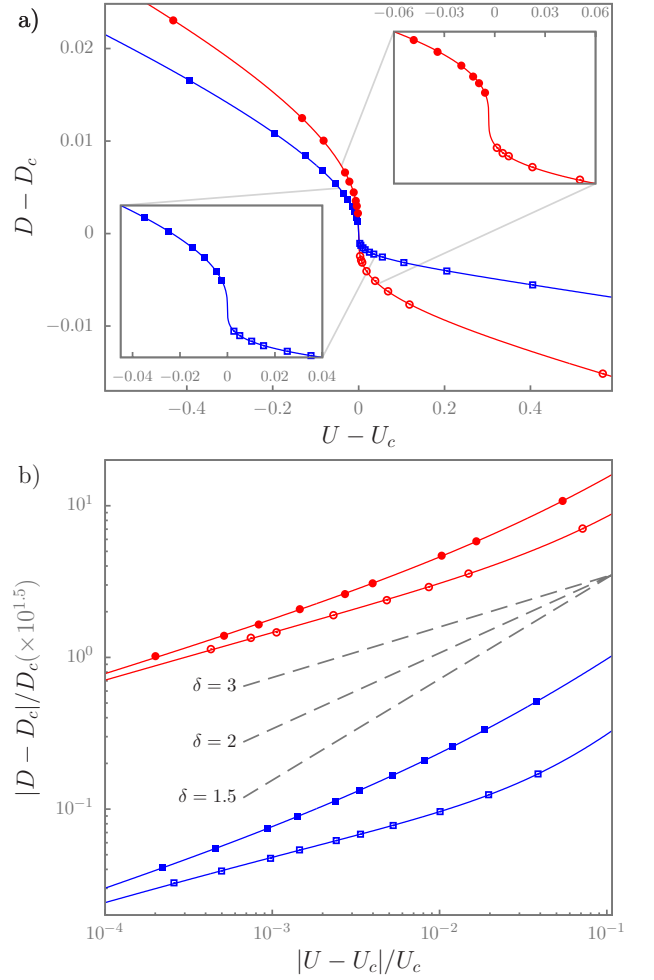


FIG. 3: Double occupancy as a function of U near the Mott critical point for the Hubbard model on an anisotropic triangular lattice with $t'/t = 0.8$ ($t \equiv 1$) at half-filling and fixed critical inverse temperature $\beta = 11.15$ (squares) for DMFT and $\beta = 9.9$ (circles) for CDMFT on a 2×2 plaquette. The solid lines show a fit to $f(U) = c_1 \text{sgn}(\delta U) |\delta U|^{1/\delta} + c_2 |\delta U|^{2/\delta} + c_3 \delta U + D_c$ ($\delta U \equiv U - U_c$) with the same parameters c_1, c_2, c_3, D_c, U_c and δ for the metallic (filled symbols) and the insulating region (open symbols). The best fitting values (U_c, D_c, δ) are (10.445, 0.0325, 2.93) for DMFT and (7.9316, 0.0679, 3.04) for CDMFT. (a) Linear plot centered at (U_c, D_c) . The insets zooms on the regions close to the critical point. (b) Logarithmic plot in reduced units relative to the critical point with CDMFT data shifted by a factor of $10^{1.5}$ along the y -axis. The dashed lines show the function $\propto |U - U_c|^{1/\delta}$ with δ as indicated. In the critical regime, up to 500 iterations are necessary for convergence in the iterative solution of the (C)DMFT equation. Once convergence is reached, we take the average over hundreds of iterations. Monte-Carlo sweeps per iteration: $6 \cdot 10^9$ for DMFT and 10^9 for CDMFT.

Both the metallic (filled symbols) and insulating (open symbols) sides are shown. The critical temperature is found as follows. Below the critical temperature, there is hysteresis and a jump in double occupancy. Above

the critical temperature, double occupancy is continuous. First we searched for the highest (lowest) temperature where hysteresis (continuity) can be checked in a reasonable time. The mean of these two temperatures is then taken as an approximation for the critical temperature.

	DMFT		CDMFT	
	δ	$ c_2/c_1 $	δ	$ c_2/c_1 $
D	2.93	1.15	3.04	0.51
$G_{loc}(\tau = \beta/2)$	2.99	0.32	3.05	0.33
$\text{Im}\Delta_{loc}(\omega_n = \pi/\beta)$	3.02	0.28	3.08	0.086
$\text{Re}\Delta_{loc}(\omega_n = \pi/\beta)$	2.87	0.79	3.02	0.75

TABLE I: Estimates of the exponent δ from a fit of Eq. 9 to the critical behavior of the double occupancy D , the local Greens function G_{loc} at $\tau = \beta/2$ and the real and imaginary parts of the local hybridization Δ_{loc} function at the lowest Matsubara frequency, as obtained by DMFT and CDMFT for the same model and parameters as in Fig. 3. The ratio $|c_2/c_1|$ indicates the weight of the subleading correction, as seen from Eq. 9.

In Fig. 3a the scale is linear whereas it is logarithmic in Fig. 3b. The solid lines are fits to the functional form suggested by Eq. (9) and by the smoothness hypothesis for D ,

$$D - D_c = c_1 \text{sgn}(\delta U) |\delta U|^{1/\delta} + c_2 |\delta U|^{2/\delta} + c_3 \delta U \quad (9)$$

where δ and the coefficients are adjustable parameters. The fits include both the metallic and the insulating sides. We find $\delta = 2.93 \pm 0.15$ for DMFT, where we know that the analytical result [5] is $\delta = 3$. For CDMFT we find $\delta = 3.04 \pm 0.25$. The errors are estimated from the values of δ at the two temperatures just below and above the critical one. The log-log plot in Fig. 3b shows that the data does not lie on a perfect straight line over the wide range of reduced units considered here. The straight dashed lines are guides to the eye that show that the exponent that we would obtain by fitting over a limited range of δU would decrease from $\delta = 3$ towards $\delta = 3/2$ as we move away from the critical point. On the metallic side, the crossover extends over a rather wide region where the the exponent is close to $\delta = 2$.

As shown in Table I, different critical quantities lead to coherent estimates of δ , whereas the importance of the subleading corrections varies strongly from case to case. Note that an asymmetry of the critical quantity between the metallic and the insulating sides, as visible in the double occupancy, indicates important subleading corrections.

Discussion: We have shown that the results of numerical calculations with both DMFT and CDMFT are consistent with $\delta = 3$ (as predicted analytically [5] for DMFT), if we include the subleading corrections in the analysis. These are particularly important if the critical

data is asymmetric in the accessible region. Otherwise, fits with a single exponent may lead to δ closer to $\delta = 2$ in the metallic phase, as observed in the organics [9, 10], and in previous CDMFT [15] calculations, where analytical results are not available. Note that in the latter calculations, the value of t'/t and the direction of approach to the critical point differ from ours. That may modify the size of the crossover region.

Extracting the pressure dependence of model parameters from band structure calculations [42], we estimate that our numerical results are as close to the critical point in reduced units as are the experiments. The value $\gamma = 1$ in these experiments is the same as the mean-field one, while $\beta = 1$ would imply that a non-singular term dominates the physics in the accessible range. Since coupling to the lattice would favor mean-field exponents [43], it would be interesting to reanalyze the experimental results by including the subleading correction to the mean-field behavior. If the coupling to the lattice is irrelevant, the exponents should eventually differ from mean-field behavior sufficiently close to the transition.

To definitely settle this issue experimentally, it would be interesting to study the two-dimensional Mott transition in frustrated optical lattices, where double occupancy is directly accessible [2]. Our derivation of the subleading correction also shows that it can possibly be relevant in more mundane cases when mean-field exponents are appropriate [44], away from the critical regime.

Acknowledgments We are indebted to D. Sénéchal, J. Schmalian, R. Fernandes, E. Fradkin, M. Sentef and E. Gull for useful discussions. This work was partially supported by NSERC, the Tier I Canada Research Chair Program (A.-M. S. T.), and Université de Sherbrooke. A.-M.S.T is grateful to the Harvard Physics Department for support and P. Sémon for hospitality during the writing of this work. Partial support was also provided by the MIT-Harvard Center for Cold Atoms. Simulations were performed using a code based on the ALPS library [45] on computers provided by CFI, MELS, Calcul Québec and Compute Canada. Portions of the hybridization expansion impurity solver developed by P. Sémon were inspired by the code gracefully provided by E. Gull and P. Werner.

-
- [1] M. Imada, A. Fujimori, and Y. Tokura, Rev. Mod. Phys. **70**, 1039 (1998), URL <http://link.aps.org/doi/10.1103/RevModPhys.70.1039>.
 - [2] R. Jordens, N. Strohmaier, K. Gunter, H. Moritz, and T. Esslinger, Nature **455**, 204 (2008), ISSN 0028-0836, URL <http://dx.doi.org/10.1038/nature07244>.
 - [3] U. Schneider, L. Hackermüller, S. Will, T. Best, I. Bloch, T. A. Costi, R. W. Helmes, D. Rasch, and A. Rosch, Science **322**, 1520 (2008),

- <http://www.sciencemag.org/content/322/5907/1520.full.pdf>, [26] T. A. Maier, M. Jarrell, T. C. Schulthess, P. R. C. Kent, and J. B. White, *Physical Review Letters* **95**, 237001 (pages 4) (2005), URL <http://link.aps.org/abstract/PRL/v95/e237001>.
- [4] C. Castellani, C. D. Castro, D. Feinberg, and J. Ranninger, *Phys. Rev. Lett.* **43**, 1957 (1979), URL <http://link.aps.org/doi/10.1103/PhysRevLett.43.1957>.
- [5] G. Kotliar, E. Lange, and M. J. Rozenberg, *Phys. Rev. Lett.* **84**, 5180 (2000), URL <http://link.aps.org/doi/10.1103/PhysRevLett.84.5180>.
- [6] S. Onoda and N. Nagaosa, *Journal of the Physical Society of Japan* **72**, 2445 (2003), URL <http://jpsj.ipap.jp/link?JPSJ/72/2445/>.
- [7] P. Limelette, A. Georges, D. Jerome, P. Wzietek, P. Metcalf, and J. M. Honig, *Science* **302**, 89 (2003), <http://www.sciencemag.org/cgi/reprint/302/5642/89.pdf>, URL <http://www.sciencemag.org/cgi/content/abstract/302/5642/89>.
- [8] S. Lefebvre, P. Wzietek, S. Brown, C. Bourbonnais, D. Jérôme, C. Mézière, M. Fourmigué, and P. Batail, *Phys. Rev. Lett.* **85**, 5420 (2000).
- [9] F. Kagawa, K. Miyagawa, and K. Kanoda, *Nature* **436**, 534 (2005), ISSN 0028-0836.
- [10] F. Kagawa, K. Miyagawa, and K. Kanoda, *Nat Phys* **5**, 880 (2009), ISSN 1745-2473, URL <http://dx.doi.org/10.1038/nphys1428>.
- [11] M. Imada, *Phys. Rev. B* **72**, 075113 (2005), URL <http://link.aps.org/doi/10.1103/PhysRevB.72.075113>.
- [12] M. Imada, T. Misawa, and Y. Yamaji, *Journal of Physics: Condensed Matter* **22**, 164206 (2010), URL <http://stacks.iop.org/0953-8984/22/i=16/a=164206>.
- [13] S. Papanikolaou, R. M. Fernandes, E. Fradkin, P. W. Phillips, J. Schmalian, and R. Sknepnek, *Physical Review Letters* **100**, 026408 (pages 4) (2008), URL <http://link.aps.org/abstract/PRL/v100/e026408>.
- [14] L. Bartosch, M. de Souza, and M. Lang, *Phys. Rev. Lett.* **104**, 245701 (2010), URL <http://link.aps.org/doi/10.1103/PhysRevLett.104.245701>.
- [15] M. Sentef, P. Werner, E. Gull, and A. P. Kampf, *arXiv:1108.0428* (????).
- [16] G. Kotliar, S. Y. Savrasov, G. Pálsson, and G. Biroli, *Phys. Rev. Lett.* **87**, 186401 (2001).
- [17] T. Maier, M. Jarrell, T. Pruschke, and M. H. Hettler, *Reviews of Modern Physics* **77**, 1027 (2005).
- [18] W. Metzner and D. Vollhardt, *Phys. Rev. Lett.* **62**, 324 (1989).
- [19] A. Georges and G. Kotliar, *Phys. Rev. B* **45**, 6479 (1992).
- [20] M. Jarrell, *Phys. Rev. Lett.* **69**, 168 (1992).
- [21] A. Georges, G. Kotliar, W. Krauth, and M. J. Rozenberg, *Rev. Mod. Phys.* **68**, 13 (1996).
- [22] G. Kotliar, S. Y. Savrasov, K. Haule, V. S. Oudovenko, O. Parcollet, and C. A. Marianetti, *Reviews of Modern Physics* **78**, 865 (pages 87) (2006), URL <http://link.aps.org/abstract/RMP/v78/p865>.
- [23] H. Terletska, J. Vučičević, D. Tanasković, and V. Dobrosavljević, *Phys. Rev. Lett.* **107**, 026401 (2011), URL <http://link.aps.org/doi/10.1103/PhysRevLett.107.026401>.
- [24] A. I. Lichtenstein and M. I. Katsnelson, *Phys. Rev. B* **62**, R9283 (2000).
- [25] O. Parcollet, G. Biroli, and G. Kotliar, *Phys. Rev. Lett.* **92**, 226402 (2004), URL <http://link.aps.org/doi/10.1103/PhysRevLett.92.226402>.
- [26] T. A. Maier, M. Jarrell, T. C. Schulthess, P. R. C. Kent, and J. B. White, *Physical Review Letters* **95**, 237001 (pages 4) (2005), URL <http://link.aps.org/abstract/PRL/v95/e237001>.
- [27] B. Kyung, S. S. Kancharla, D. Sénéchal, A.-M. S. Tremblay, M. Civelli, and G. Kotliar, *Physical Review B (Condensed Matter and Materials Physics)* **73**, 165114 (pages 6) (2006), URL <http://link.aps.org/abstract/PRB/v73/e165114>.
- [28] B. Kyung and A.-M. S. Tremblay, *Physical Review Letters* **97**, 046402 (pages 4) (2006), URL <http://link.aps.org/abstract/PRL/v97/e046402>.
- [29] K. Haule and G. Kotliar, *Physical Review B (Condensed Matter and Materials Physics)* **76**, 104509 (pages 37) (2007), URL <http://link.aps.org/abstract/PRB/v76/e104509>.
- [30] S. S. Kancharla, B. Kyung, D. Senechal, M. Civelli, M. Capone, G. Kotliar, and A.-M. S. Tremblay, *Physical Review B (Condensed Matter and Materials Physics)* **77**, 184516 (pages 12) (2008), URL <http://link.aps.org/abstract/PRB/v77/e184516>.
- [31] T. Ohashi, T. Momoi, H. Tsunetsugu, and N. Kawakami, *Physical Review Letters* **100**, 076402 (pages 4) (2008), URL <http://link.aps.org/abstract/PRL/v100/e076402>.
- [32] S. Sakai, Y. Motome, and M. Imada, *Phys. Rev. Lett.* **102**, 056404 (2009), URL <http://link.aps.org/doi/10.1103/PhysRevLett.102.056404>.
- [33] A. Liebsch and N.-H. Tong, *Phys. Rev. B* **80**, 165126 (2009), URL <http://link.aps.org/doi/10.1103/PhysRevB.80.165126>.
- [34] A. Liebsch, H. Ishida, and J. Merino, *Phys. Rev. B* **79**, 195108 (2009), URL <http://link.aps.org/doi/10.1103/PhysRevB.79.195108>.
- [35] G. Sordi, K. Haule, and A. M. S. Tremblay, *Phys. Rev. Lett.* **104**, 226402 (2010).
- [36] P. Werner, A. Comanac, L. de' Medici, M. Troyer, and A. J. Millis, *Phys. Rev. Lett.* **97**, 076405 (2006).
- [37] P. Werner and A. J. Millis, *Physical Review B (Condensed Matter and Materials Physics)* **74**, 155107 (pages 13) (2006), URL <http://link.aps.org/abstract/PRB/v74/e155107>.
- [38] E. Gull, A. J. Millis, A. I. Lichtenstein, A. N. Rubtsov, M. Troyer, and P. Werner, *Rev. Mod. Phys.* **83**, 349 (2011), URL <http://link.aps.org/doi/10.1103/RevModPhys.83.349>.
- [39] K. Haule, *Physical Review B (Condensed Matter and Materials Physics)* **75**, 155113 (pages 12) (2007).
- [40] M. Potthoff, *Eur. Phys. J. B (France)* **32**, 429 (2003).
- [41] G. Kotliar, *The European Physical Journal B - Condensed Matter and Complex Systems* **11**, 27 (1999), ISSN 1434-6028, 10.1007/s100510050914, URL <http://dx.doi.org/10.1007/s100510050914>.
- [42] H. C. Kandpal, I. Opahle, Y.-Z. Zhang, H. O. Jeschke, and R. Valentí, *Phys. Rev. Lett.* **103**, 067004 (2009), URL <http://link.aps.org/doi/10.1103/PhysRevLett.103.067004>.
- [43] T. Chou and D. R. Nelson, *Phys. Rev. E* **53**, 2560 (1996).
- [44] R. Brout, *Phys. Rev.* **118**, 1009 (1960), URL <http://link.aps.org/doi/10.1103/PhysRev.118.1009>.
- [45] A. A. et al., *J. Magn. Magn. Mater.* **310**, 1187 (2007).